

Subtractive renormalization of the NN scattering amplitude at leading order in chiral effective theory

C.-J. Yang, Ch. Elster, and D. R. Phillips

*Institute of Nuclear and Particle Physics,
and Department of Physics and Astronomy, Ohio University,
Athens, OH 45701**

(Dated: February 1, 2008)

The leading-order nucleon-nucleon (NN) potential derived from chiral perturbation theory consists of one-pion exchange plus short-distance contact interactions. We show that in the 1S_0 and 3S_1 – 3D_1 channels renormalization of the Lippmann-Schwinger equation for this potential can be achieved by performing one subtraction. This subtraction requires as its only input knowledge of the NN scattering lengths. This procedure leads to a set of integral equations for the partial-wave NN t-matrix which give cutoff-independent results for the corresponding NN phase shifts. This reformulation of the NN scattering equation offers practical advantages, because only observable quantities appear in the integral equation. The scattering equation may then be analytically continued to negative energies, where information on bound-state energies and wave functions can be extracted.

PACS numbers: 12.39.Fe, 25.30.Bf, 21.45.+v

I. INTRODUCTION

Chiral perturbation theory (χ PT) [1, 2, 3] provides a systematic technique by which nuclear forces can be derived. As first pointed out by Weinberg [4, 5], the nucleon-nucleon (NN) potential can be expanded in powers of the χ PT expansion parameter $P \equiv \frac{p \cdot m_\pi}{\Lambda_\chi}$. The leading-order (LO= P^0) potential is then the venerable one-pion exchange (OPE), supplemented by a short-distance “contact interaction”, which is a constant in momentum space, or equivalently in co-ordinate space a three-dimensional delta function. Thus, the LO χ PT potential is singular, and when iterated in a Lippmann-Schwinger (LS) equation requires regularization and renormalization.

Weinberg’s idea has since been extended to several orders in the chiral expansion with NN potentials of χ PT derived to NNLO in Refs. [6, 7, 8] and to N³LO [9, 10]. At N³LO a fit to NN data below $T_{\text{lab}} = 200$ MeV can be achieved which is comparable in quality to that obtained in ‘high-quality’ NN potential models, provided cutoffs in the range 500–600 MeV are considered [9]. For this cutoff range the phase shifts obtained from the N³LO χ PT potential have little residual cutoff dependence at $T_{\text{lab}} \leq 200$ MeV.

However, cutoff independence over a wider range is desirable. In field-theoretic terms the issue of whether this can be achieved or not speaks to whether a single momentum-independent contact interaction is sufficient to renormalize the singular OPE potential [11, 12]. Beane, Bedaque, Savage, and van Kolck imposed a co-ordinate space regulator on the LO χ PT potential, and adjusted the two free parameters that multiply the contact interactions so as to reproduce both S-wave NN scattering lengths. They then showed that the resulting phase shifts are independent of the regulator scale (up to small higher-order corrections) when it is varied over an order of magnitude [13]. (Ref. [13] also showed that renormalization of the m_π -dependence of the nuclear force requires the contact interaction to be a function of m_π , but such m_π -dependence will not concern us here.) This cutoff-independence of NN S-wave phase shifts resulting from the LO potential derived by Weinberg has since been confirmed by Ruiz Arriola and Pavon Valderrama [14], and—using a momentum-space cutoff—by Nogga, Timmermans and van Kolck [15]. In addition, Ref. [15] examined the behavior of this LO potential in higher partial waves and argued that channels with $l \geq 1$ in which the OPE potential is attractive also need additional contact interactions if they are to be properly renormalized, a finding which was confirmed in Ref. [16]. This analysis agrees with an examination of the renormalization-group scaling of short-distance operators in the presence of one-pion exchange [17]. The usefulness of the results of Refs. [15, 16, 17] has, however, been disputed in Ref. [18]. For a review of the situation see Ref. [19].

*Electronic address: cjyang, elster, phillips@phy.ohiou.edu

However, the NN partial waves on which this ongoing discussion centers are not the focus of this study. Instead, we will re-examine the renormalization of the leading-order χ PT potential in the 1S_0 and 3S_1 - 3D_1 channels. We will develop a strategy that replaces the divergent integrals and unphysical contact interactions that appear in the LS equation for this potential with finite integrals and physical quantities. In particular, we will show that knowledge of the zero-energy on-shell NN scattering amplitude allows us to turn an ill-behaved LS equation into a set of equations that give cutoff-independent results which are equivalent to the ones obtained in Ref. [15].

Such a conversion of divergent loop integrals and potentially infinite Lagrangian couplings into a sum of experimental quantities and convergent integrals is a well-known strategy in perturbation theory. In a renormalizable theory it was shown to be possible to pursue this strategy to all orders in perturbation theory by Bogoluibov, Parasuik, Hepp, and Zimmerman [20]. Hereafter we refer to this approach as “subtractive” renormalization. We show that such subtractive renormalization can be applied to the LS equation for the LO χ PT potential. This is a non-trivial result, as while contact interactions have simple integral representations in perturbation theory the contact terms appearing in the LO χ PT potential do not. In consequence the development of subtractive renormalization in a non-perturbative context is, to our knowledge, only a recent advance, having been originally developed for the “pionless EFT” in Refs. [21, 22].

An earlier attempt to develop subtractive renormalization for the NN interaction of χ PT was made in Ref. [23], and extended in Ref. [24]. There a large negative energy, $E_{sub} = -\frac{\mu^2}{M}$, is used as subtraction point while solving the LS equation at a fixed c.m. energy in the NN system. The assumption that the Born approximation holds at E_{sub} , provided the parameter μ is large enough, then determines the behavior of the NN amplitude at that energy. However, this assumption is not generally valid for a singular potential. Frederico *et al.* therefore effectively enforce a particular off-shell dependence of the t-matrix at E_{sub} . We will show that such an assumption is not necessary. Instead, subtractions first suggested by Hammer and Mehen [21] can be used at $E = 0$ to obtain the half-shell NN t-matrix $t(p, 0; E = 0)$ from the original LS equation and the NN scattering length. From this, NN phase shifts at any energy can be obtained assuming only Hermiticity of the underlying potential. The latter technique was developed and employed by Afnan and Phillips [22] in the context of the low-energy three-body problem, but was not yet used in a two-body context.

The paper is structured as follows. In Section II we review the LO χ PT NN potential and solve the LS equation for S-waves employing a momentum cutoff. We demonstrate the well-known result that S-wave phase shifts are cutoff dependent unless the contact interaction is adjusted so as to reproduce some low-energy observable. We reproduce the results of Ref. [15] for cutoffs in the range 0.5 to 4 GeV. In Sec. III we perform subtractions on the LS equation such that reference to the contact interaction disappears and demonstrate that this procedure results in cutoff-independent predictions for NN phase shifts. Our use of subtractive renormalization allows us to consider cutoffs that are much larger than those used in Ref. [15], and in Sec. III we consider Λ as high as 50 GeV in order to show what is possible with our new technique. We also explain the differences between our approach and that of Ref. [23]. In Sec. IV we analytically continue the subtracted equation to negative energies and obtain bound-state energies and wave functions, thereby showing that our techniques are equally suitable for obtaining the NN bound state energy and wave function. We summarize and outline possible extensions of this work in Sec. V.

II. THE LEADING-ORDER NN POTENTIAL IN CHIRAL PERTURBATION THEORY

As first pointed out by Weinberg in Refs. [4, 5], in χ PT the operators of lowest chiral dimension which can contribute to the NN potential are:

$$\langle \mathbf{p}' | V | \mathbf{p} \rangle = -\tau_1 \cdot \tau_2 \frac{g_A^2}{4f_\pi^2} \frac{\sigma_1 \cdot (\mathbf{p}' - \mathbf{p}) \sigma_2 \cdot (\mathbf{p}' - \mathbf{p})}{(\mathbf{p}' - \mathbf{p})^2 + m_\pi^2} + \pi[(C_T + 3C_S) + \tau_1 \cdot \tau_2(C_S - C_T)] \quad (2.1)$$

where τ_1, τ_2 are the isospin and σ_1, σ_2 the spin operators. The couplings constants are given by $g_A = 1.25$ and $f_\pi = 93$ MeV, the c.m. momentum by \mathbf{p} . The low-energy constants C_S and C_T represent the effects of degrees of freedom with masses of order Λ_χ . Their value is not determined by chiral symmetry, and they must be fitted to experimental or lattice [25] data. Weinberg then advocated inserting this potential into the non-relativistic Lippmann-Schwinger equation, which is sufficient because we are considering a low-energy expansion of V :

$$\langle \mathbf{p}' | t(E) | \mathbf{p} \rangle = \langle \mathbf{p}' | V | \mathbf{p} \rangle + \int \frac{d^3 p''}{(2\pi)^3} \langle \mathbf{p}' | V | \mathbf{p}'' \rangle \frac{1}{E + i\varepsilon - \frac{p''^2}{M}} \langle \mathbf{p}'' | t(E) | \mathbf{p} \rangle \quad (2.2)$$

(with ε a positive infinitesimal and M the nucleon mass). This resums the effects of infra-red enhancement due to the presence of heavy (c.f. m_π) particles in the intermediate NN state. In a partial-wave expansion Eq. (2.2) reads

$$t_{\nu l}(p', p; E) = v_{\nu l}(p', p) + \sum_{\nu''} \frac{2}{\pi} M \int_0^\infty \frac{dp'' p''^2 v_{\nu \nu''}(p', p'') t_{\nu'' l}(p'', p, E)}{p_0^2 + i\varepsilon - p''^2}, \quad (2.3)$$

where $p_0^2/M = E$ is the c.m. energy, and l denotes the angular-momentum quantum number. For the singlet state we have $l = l' = l'' = 0$, for the triplet state these values can be 0 or 2. The explicit expressions for the partial wave projections of OPE are given in Ref. [23]. For the convenience of the reader we repeat them here. For the 1S_0 state one obtains (with $C_T, C_S = 0$)

$$v_{00}^s(p', p) = \frac{g_A^2}{32\pi f_\pi^2} \left(2 - \int_{-1}^1 dx \frac{m_\pi^2}{p'^2 + p^2 - 2p'px + m_\pi^2} \right). \quad (2.4)$$

The angular-momentum projected matrix elements for the 3S_1 - 3D_1 channels ($l, l' = 0, 2$) are given by

$$\begin{aligned} v_{00}^t(p', p) &= \frac{g_A^2}{32\pi f_\pi^2} \left(2 - \int_{-1}^1 dx \frac{m_\pi^2}{p'^2 + p^2 - 2p'px + m_\pi^2} \right) \\ v_{20}^t(p', p) &= \frac{g_A^2 \sqrt{2}}{16\pi f_\pi^2} \left(\int_{-1}^1 dx \frac{p'^2 - 2p'px + p^2(\frac{3}{2}x^2 - \frac{1}{2})}{p'^2 + p^2 - 2p'px + m_\pi^2} \right) \\ v_{22}^t(p', p) &= \frac{g_A^2}{32\pi f_\pi^2} \left(\int_{-1}^1 dx \frac{2pp'x - (p^2 + p'^2)(\frac{3}{2}x^2 - \frac{1}{2})}{p'^2 + p^2 - 2p'px + m_\pi^2} \right). \end{aligned} \quad (2.5)$$

Inspection of the limits for $p, p' \rightarrow \infty$ for $v_{00}(p', p)$ in Eq. (2.4) gives [23]

$$\lim_{p \text{ or } p' \rightarrow \infty} v_{00}^s(p', p) = \frac{g_A^2}{16\pi f_\pi^2}. \quad (2.6)$$

For the triplet channels the following limits give a finite value [23]

$$\begin{aligned} \lim_{p \text{ or } p' \rightarrow \infty} v_{00}^t(p', p) &= \frac{g_A^2}{16\pi f_\pi^2}, \\ \lim_{p' \rightarrow \infty} v_{20}^t(p', p) &= \frac{g_A^2 \sqrt{2}}{8\pi f_\pi^2}, \end{aligned} \quad (2.7)$$

while $\lim_{p \rightarrow \infty} v_{20}^t(p', p) = \lim_{p, p' \rightarrow \infty} v_{22}^t(p', p) = 0$. Thus, the integrals of Eq. (2.3) diverge. The ultra-violet behavior of the integral equation can be regulated by introducing a momentum cutoff Λ as the upper bound of the integration. Meanwhile, the infra-red singularity at $p = p_0$ in Eq. (2.3) is separated into a principal-value part and a delta-function part, with the principal-value singularity treated by standard subtraction techniques [26].

Once these two steps are made the integral equation can be solved by standard Gauss-Legendre quadrature. The results of our numerical calculations for the 1S_0 and 3S_1 - 3D_1 phase shifts are shown on the left-hand side of Figs. 1. We confirm that if $C_S(C_T)$ takes a fixed value (e.g. zero), the resulting 1S_0 (3S_1) phase shift has sizable cutoff variation—of order δ_{1S_0} (δ_{3S_1}) itself—even for small projectile laboratory energies T_{lab} .

One way to remedy the situation is to renormalize each of the S-wave potentials by taking advantage of the presence of the arbitrary constants C_S and C_T . In Ref. [15] Eq. (2.2) was solved with the relevant constant adjusted such that for a given cutoff Λ the S-wave phase shifts at 10 MeV were reproduced. Here we do something similar, except that we use the NN scattering lengths as input, adopting the values $a_s = -23.7$ fm for the singlet case and $a_t = 5.43$ fm for the triplet [27].

Once C_S and C_T are fitted in this way we can predict the phase shift at an arbitrary energy, and the resulting “renormalized” phase shifts are plotted in the right-hand panels of Figs. 1 as a function of the laboratory kinetic energy. The phase shifts are now approximately cutoff independent, with the dependence on Λ relegated to effects $\sim 1/\Lambda$ in the effective ranges, r_s and r_t (see Table I). This reproduces results of Beane, Bedaque, Savage and van Kolck and others [13, 15].

The renormalization constants C_S and C_T that were used to generate these results are given in Table II together with the corresponding cutoff Λ . While C_S exhibits a monotonic behavior as function of Λ , the evolution of C_T with Λ is particularly interesting, and is shown in Fig. 2. This confirms the result shown in Fig. 2 of Ref. [15], and shows that $C_T(\Lambda)$ diverges at specific values of Λ . The origin of this behavior is the appearance of additional bound states in the 3S_1 - 3D_1 channel as the cutoff is increased. At the specific values of Λ where one more bound state appears, Eq. (2.2) cannot be solved by fitting $C_T(\Lambda)$ to reproduce a_t .

But even when the constants $C_{T(S)}$ are finite, fitting them in order to reproduce the scattering length can be very delicate. For example, at $\Lambda = 1$ GeV C_S must be tuned to 1 part in 10^4 in order to get a_s accurate to 1%, while for $\Lambda = 10$ GeV it must be tuned to 1 part in 10^6 to achieve this accuracy. At arbitrarily large cutoffs it therefore becomes numerically impossible to fit C_S and C_T .

III. SUBTRACTED INTEGRAL EQUATIONS

An alternative to fitting the contact interactions C_S and C_T so as to reproduce the 1S_0 and 3S_1 scattering lengths is to perform subtractive renormalization on the LS equations for the potential (2.1). In this section we explain the subtractive renormalization procedure. Note that in contrast to the approach advocated in Ref. [23], our subtraction procedure does not require assumptions about the behavior of t anywhere.

Let us first concentrate on the c.m. energy $E = 0$ in the NN system. The definition of the scattering lengths $a_{s(t)}$ in the limit $E \equiv p_0^2/M \rightarrow 0$ gives in the singlet (triplet) states

$$t_{00}^{s(t)}(0, 0, E = 0) = \frac{f_{00}^{s(t)}(0)}{-Mp_0} = \frac{a_{s(t)}}{M}, \quad (3.1)$$

where $f_{00}^{s(t)}(E)$ represents the scattering amplitude in the singlet (s) or triplet (t) channel. The half-shell and on-shell LS equations for this energy read

$$t(p, 0; 0) = v(p, 0) + C + \frac{2}{\pi} M \int_0^\Lambda dp' p'^2 \left(\frac{v(p, p') + C}{-p'^2} \right) t(p', 0; 0) \quad (3.2)$$

$$t(0, 0; 0) = v(0, 0) + C + \frac{2}{\pi} M \int_0^\Lambda dp' p'^2 \left(\frac{v(0, p') + C}{-p'^2} \right) t(p', 0; 0), \quad (3.3)$$

where we dropped the channel indices since our procedure is valid for the singlet as well as triplet LS equations. Subtracting Eq. (3.3) from Eq. (3.2) and using (3.1) leads to

$$t_{00}^s(p, 0; 0) = v_{00}^s(p, 0) + \frac{a_s}{M} + \frac{2}{\pi} M \int_0^\Lambda dp' p'^2 \left(\frac{v_{00}^s(p, p') - v_{00}^s(0, p')}{-p'^2} \right) t_{00}^s(p', 0; 0) \quad (3.4)$$

in the singlet channel, while for the triplet channel the equation corresponding to Eq. (3.4) is

$$t_{l'l'}^t(p', 0; 0) - \sum_{l''} \frac{2}{\pi} M \int_0^\Lambda dp'' p''^2 \left(\frac{v_{l'l''}^t(p', p'') - v_{l'l''}^t(0, p'')}{-p''^2} \right) t_{l''l'}^t(p'', 0; 0) = v_{l'l'}^t(p', 0) - v_{l'l'}^t(0, 0) + \delta_{l'0} \delta_{l0} \frac{a_t}{M}, \quad (3.5)$$

where $l, l' = 0, 2$. Note that since $v_{20}(0, p; 0) = v_{02}(p, 0; 0) = 0$, and $v_{22}(0, p; 0) = v_{22}(p, 0; 0) = 0$, the corresponding t-matrix elements t_{02} and t_{22} must also be zero.

Equations akin to Eqs. (3.4) and (3.5) were first developed for the three-body problem in Ref. [21]. They have the advantage that the constants C_S and C_T cancel out in the differences that form Eqs. (3.4) and (3.5), so that these equations contain only observable quantities. They can be solved using standard techniques. Our results shows the relative difference between the two methods is less than 0.2% for all channels.

Having determined $t(p, 0; 0)$ we set about obtaining half-shell t-matrix elements $t(p, p'; 0)$, p' being an arbitrary momentum, by carrying out a further subtraction. First we note that:

$$t(p, p'; 0) = v(p, p') + C + \frac{2}{\pi} M \int_0^\Lambda dp'' p''^2 \left(\frac{v(p, p'') + C}{-p''^2} \right) t(p'', p'; 0) \quad (3.6)$$

$$t(0, p'; 0) = v(0, p') + C + \frac{2}{\pi} M \int_0^\Lambda dp'' p''^2 \left(\frac{v(0, p'') + C}{-p''^2} \right) t(p'', p'; 0). \quad (3.7)$$

Subtracting Eq. (3.7) from Eq. (3.6) leads to

$$t(p, p'; 0) - t(0, p'; 0) = v(p, p') - v(0, p') + \frac{2}{\pi} M \int_0^\Lambda dp'' p''^2 \left(\frac{v(p, p'') - v(0, p'')}{-p''^2} \right) t(p'', p'; 0). \quad (3.8)$$

Taking advantage of the property $t(p', 0; 0) = t(0, p'; 0)^T$, we can use $t(p', 0; 0)$ obtained from Eq. (3.5) to solve for $t(p, p'; 0)$ in Eq. (3.8). The calculated results are displayed in Fig. 3 and show good agreement (relative difference $\leq 2\%$) between this subtractive method and the one described in the previous section.

As a last step we need to obtain the general half-shell t-matrix $t(p, p'; E)$ at arbitrary c.m. energies E from the one at zero energy that is given by Eq. (3.8). We start again from two LS equations,

$$t(p, p'; 0) = v(p, p') + C + \frac{2}{\pi} M \int_0^\Lambda dp'' p''^2 \left(\frac{v(p, p'') + C}{-p''^2} \right) t(p', p''; 0). \quad (3.9)$$

$$t(p, p'; E) = v(p, p') + C + \frac{2}{\pi} M \int_0^\Lambda dp'' p''^2 \left(\frac{v(p, p'') + C}{p_0^2 - p''^2 + i\epsilon} \right) t(p', p''; E), \quad (3.10)$$

which, in order to express the idea more clearly, we simplify to

$$t(0) = (v + C) + (v + C)g(0)t(0), \quad (3.11)$$

$$t(E) = (v + C) + (v + C)g(E)t(E). \quad (3.12)$$

The second equation, Eq. (3.12), can be rewritten as

$$t(E)(1 + g(E)t(E))^{-1} = v + C, \quad (3.13)$$

whereas the first, Eq. (3.11), can also be expressed as

$$t(0) = (v + C) + t(0)g(0)(v + C). \quad (3.14)$$

Substituting Eq. (3.13) into Eq. (3.14) gives

$$t(0) = [1 + t(0)g(0)] t(E) [1 + g(E)t(E)]^{-1}, \quad (3.15)$$

which after simplification yields

$$t(E) = t(0) + t(0)(g(E) - g(0))t(E). \quad (3.16)$$

We can now obtain $t(E)$ from $t(0)$ by solving the integral equation, Eq. (3.16). Then choosing $p = p_0$ with $E = p_0^2/M$ and setting $p' = p$ we have the on-shell t-matrix element $t_l(p_0, p_0; E)$ at an arbitrary energy E . The on-shell element is related to the phase shift δ_l through the well-known relation

$$t_l(p_0, p_0; E) = -\frac{e^{i\delta_l} \sin \delta_l}{Mp_0}. \quad (3.17)$$

The 1S_0 phase shifts calculated in this way is shown in the upper left panel of Fig. 4, where they are compared to those found by fitting C_S , as described in the previous section. The agreement between the two methods is very good, which confirms the ability of the subtraction to reproduce the results obtained by fitting C . The phase shifts produced by the CD-Bonn potential [28] are also shown in Fig. 4. Since this potential reproduces the NN data in this region with $\chi^2/\text{d.o.f} \approx 1$ its δ_{1S_0} can be regarded as a parameterization of experiments. But the CD-Bonn values for δ_{1S_0} are not well reproduced by the LO χ PT potential. In this channel the LO calculation obviously has sizable higher-order corrections. In fact the description is known to improve when additional terms in the chiral expansion of V are included [6, 8, 29].

Meanwhile the other three panels of Fig. 4 show results for the triplet channel, where we adopt the Stapp convention [30] for the phase shifts and the mixing parameter

$$\begin{aligned} \epsilon &= \frac{1}{2} \arctan \left[\frac{-i(t_{02}^t + t_{20}^t)}{2\sqrt{t_{00}^t t_{22}^t}} \right] \\ \delta(^3S_1) &= \frac{1}{2} \arctan \left[\frac{\Im[(t_{00}^t)/\cos(2\epsilon)]}{\Re[(t_{00}^t)/\cos(2\epsilon)]} \right] \\ \delta(^3D_1) &= \frac{1}{2} \arctan \left[\frac{\Im[(t_{22}^t)/\cos(2\epsilon)]}{\Re[(t_{22}^t)/\cos(2\epsilon)]} \right]. \end{aligned} \quad (3.18)$$

The agreement between the two methods employed to perform the LO χ PT calculation of these quantities is satisfactory, and for δ_{3S_1} and δ_{3D_1} the agreement of the LO calculation with the CD-Bonn phases is strikingly good.

The main numerical challenge of our subtractive renormalization scheme originates in solving Eq. (3.8) and Eq. (3.16). Matrix elements with large p' are small and in the subtraction scheme they are calculated from a combination of larger matrix elements. We now compare the efficiency of the subtraction and fitting methods. We first note that due to the multi-step nature of subtraction, it does take about 3 times longer to run the code than it does for the fitting method with the same number of mesh points. On the other hand, as Table III shows, the subtraction method converges much faster than the fitting method with respect to the number of mesh points used in the calculation. With 20 mesh points we already have 4 significant-figure accuracy for the subtraction method, while to reach this accuracy it takes more than 200 mesh points for the fitting method. The subtraction method converges so much faster because in the fitting method C_T affects only the part of the off-shell amplitude near $p = \Lambda$, and the oscillation phase it sets there must be communicated down to $p = 0$ to get a particular scattering length a_t . In the subtraction method the correct value of the scattering length is enforced in the equation itself, and does not

have to be achieved by fine tuning the constant C_T so as to obtain the correct behavior of the half-off-shell amplitude for p of order Λ .

For the same number of mesh points, converged phase shifts calculated by the two different methods differ by 0.1–1.3% depending on the energy, as is shown in Fig. 5. The mixing parameter for the triplet channel is more sensitive to numerical errors, and in that quantity there is a 1–2% relative difference between the two methods. However, we still claim that both methods are equivalent.

Frederico *et al.* also follow the steps around Eqs. (3.11) and (3.12), although there the difference of t-matrices is constructed between a given c.m. energy E of the NN system and a large negative energy $-\frac{\mu^2}{M}$ [23]. (See also Refs. [31, 32], where similar “first-resolvent” methods are employed.) Taking $\mu = 0$ in Eq. (8) of Ref. [23] yields our Eq. (3.16). The difference between that work and what we have done here is that in Ref. [23] the Born approximation $t = V$ with V given by Eq. (2.1) is used to determine $t(-\frac{\mu^2}{M})$. The final results are then independent of the “subtraction point” μ , provided that μ is large enough. This procedure leads to numerical results for phase shifts which are similar to ours. But it relies on the validity of the Born approximation at large negative energies. Since the tensor potential that operates in the triplet channel $\sim \frac{1}{r^3}$ at short distances the Born approximation is not actually valid at any energy [33, 34].

We can see this failure of the Born approximation in the triplet channel by examining the off-shell t-matrix at a number of negative energies $E = -\frac{\mu^2}{M}$ and comparing the results to V itself. Fig. 6 shows that the behavior of $t_t(p, p'; -\frac{\mu^2}{M})$ at fixed p' is completely different from the behavior of V . (In contrast, in the singlet channel the Born approximation appears to work quite well if μ is large enough.) This defect in Frederico *et al.*’s argument is manifested in the fact that μ dependence in physical quantities disappears only slowly as $\mu \rightarrow \infty$. The mixing parameter ϵ_1 , which is particularly sensitive to the tensor potential, is one significant example of this. Our subtraction method gives quite good convergence of ϵ_1 with respect to cutoff, as shown in Fig. 7, and the convergence of other physical quantities with respect to Λ as $\Lambda \rightarrow \infty$ is quite rapid, see Tables I–II (c.f. Table 1 of Ref. [23]). This presumably results from the fact that our subtractive renormalization of the LS equation is based only on Hermiticity of the potential and momentum-independence of the contact interaction C . Under these assumptions all the results of this section and Sec. IV below are determined by the form of one-pion exchange and the value of the NN scattering lengths that are supplied in Eqs. (3.4) and (3.5).

IV. SUBSTRUCTIVE RENORMALIZATION IN BOUND-STATE CALCULATIONS

The neutron and proton form a bound state in the 3S_1 - 3D_1 partial-wave state: the deuteron. In this section we review the methods by which the deuteron binding energy is deduced from the NN t-matrix, and employ the t-matrix obtained via subtractive renormalization in the previous section to obtain NN binding energies and wave functions.

Let us consider the Schrödinger equation

$$H\psi = E\psi = -B\psi \quad (4.1)$$

with $H = H_0 + V$, $H_0 = \frac{p^2}{M}$ the free Hamiltonian, V the previously renormalized potential, and B the unknown binding energy. By rearranging and partial-wave expanding Eq. (4.1) and defining:

$$\langle p|\Gamma_l\rangle = (-B - \frac{p^2}{M})\langle p|\psi_l\rangle = \langle p|(-B - H_0)|\psi_l\rangle \equiv \langle p|g^{-1}(-B)|\psi_l\rangle, \quad (4.2)$$

we obtain

$$\langle p|\Gamma_l\rangle = \frac{2}{\pi} \int dp' p'^2 v_{ll'}(p, p') \frac{1}{-B - \frac{p'^2}{M}} \langle p'|\Gamma_{l'}\rangle. \quad (4.3)$$

The kernel $v_{ll'}(p, p') (-B - \frac{p'^2}{M})^{-1}$ of Eq. (4.3) is the same as the kernel of the equation for the t-matrix (2.3). We see from Eq. (4.3) that the kernel will have an eigenvalue $\lambda(E) = 1$ when the energy is equal to that at which a bound-state occurs, $E = -B$. Thus by varying B and solving the eigenvalue problem we can obtain the binding energy. If the constant C_T is fit to a scattering length of $a_t = 5.43$ fm we obtain $B = 2.13$ MeV for $\Lambda = 50000$ MeV. In Table IV the values of $B \equiv B_{fit}$ for different cutoff parameters are listed. We note that for small cutoff parameters Λ , the fitting procedure leads to a slightly larger value of B_{fit} . In Fig. 8 the trend of eigenvalues λ_e is shown as a function of B_{fit} for $\Lambda = 50000$ MeV, and we see that the deuteron is actually the 8th excited state of the system for this cutoff. As $\Lambda \rightarrow \infty$ the number of bound states in the NN system increases monotonically, but renormalization ensures that the shallowest one is always at $B \approx 2$ MeV.

We now want to demonstrate that we can apply the approach discussed in Sec. 3 to the bound-state problem. Multiplying Eq. (3.16) with $(E + B)$ we obtain

$$(E + B) t(E) = t(0) \left[(E + B) + (g(E) - g(0)) (E + B) t(E) \right] \quad (4.4)$$

When considering the bound state, i.e. $E \rightarrow -B$, the first term in the brackets on the right-hand side vanishes. But, since, the t-matrix has a pole at $E = -B$, we can define the residue at the pole as $f(-B) = \lim_{E \rightarrow -B} (E + B) t(E)$. Consequently, upon taking the limit, Eq. (4.4) becomes

$$f(-B) = t(0) \left[g(-B) - g(0) \right] f(-B) \equiv t(0) \left[\frac{1}{-H_0 - B} - \frac{1}{-H_0} \right] f(-B). \quad (4.5)$$

If this equation is written for the partial-wave form of the t-matrix then the residue operator $f_{ll'}(-B)$ is related to the function $\langle p | \Gamma_l \rangle$ of Eq. (4.3) by

$$\langle p | \Gamma_l \rangle \langle \Gamma_{l'} | p' \rangle = \langle p | f_{ll'}(-B) | p' \rangle. \quad (4.6)$$

We already calculated $t(0)$ in Section 3, thus the kernel of Eq. (4.5) can be evaluated directly. The energy $E = -B$ at which it has an eigenvalue of 1 reveals the bound-state energy, and the eigenvector is then the function $\langle p | \Gamma_l \rangle$ (up to an overall constant). Our numerical calculation gives a deuteron binding energy $B \equiv B_{sub} = 2.11$ MeV. This result is independent of the cutoff to better than 0.5% for $\Lambda > 500$ MeV (see Table IV). The relative difference in the binding energy of the shallowest state obtained by solving Eq. (4.3) and Eq. (4.5) is 0.94% for $\Lambda = 50000$ MeV. From this we conclude that the subtractive renormalization works for the bound state as well (or better) than it does for scattering observables. Fig. 9 shows the trend of eigenvalues λ_e of the kernel of Eq. (4.5) as a function of B_{sub} . Our calculation gives a deuteron binding energy different from the experimental value $B_{exp} = 2.2246$ MeV. The reason for this difference is that we work only with the LO χ PT potential, and so the analytic continuation of the scattering amplitude from the scattering to the bound-state regime is only accurate up to corrections of order $\frac{(p, m_\pi)^2}{\Lambda_\chi^2}$.

In spite of this discrepancy with experiment we can still check that our eigenenergy is the correct one for LO χ PT with the experimental value of a_t reproduced. To do this we use the S-wave effective-range expansion for the on-shell t-matrix t_{00}^t ,

$$-M t_{00}^t = \frac{1}{-\frac{1}{a_t} + \frac{1}{2} r_t p_0^2 - i p_0}, \quad (4.7)$$

with r_t being the triplet effective range. This form of t_{00}^t is valid for on-shell momenta p_0 that obey $|p_0| < m_\pi/2$. The pole in the t-matrix representing the shallowest bound state of the NN system is inside this radius of convergence. Thus we can solve

$$\frac{1}{a_t} - \frac{1}{2} r_t p_0^2 + i p_0 = 0 \quad (4.8)$$

for $p_0 = i\gamma$ in order to determine its location, and B is then equal to γ^2/M . Using the experimental value of a_t , and the value of r_t extracted from our phase shifts, we obtain $B = 2.07$ MeV. This value has a relative difference of $\sim 1\%$ with respect to the two previously calculated values. This is consistent with the omission of terms of $O(p_0^4)$ in the effective-range expansion form employed in Eq. (4.7). We now turn to extraction of the deuteron wave function. In a particular partial wave this is related to the above defined function $\langle p | \Gamma_l \rangle$ via

$$\psi_l(p) = -\frac{1}{B + \frac{p^2}{M}} \langle p | \Gamma_l \rangle. \quad (4.9)$$

Since $\langle p | \Gamma_l \rangle$ is equal to the eigenvector, up to an overall constant, it is now a simple matter to obtain $\psi_l(p)$. In the upper part of Fig. 10 the momentum-space S-wave and D-wave calculated from the above subtraction method are compared with those obtained from the CD-Bonn potential. The overall constant is fixed by our normalization condition

$$\int dp p^2 [\psi_0^2(p) + \psi_2^2(p)] = 1. \quad (4.10)$$

Here $\psi_0(\psi_2)$ is the $^3S_1(^3D_1)$ wave function. The agreement of the LO χ PT momentum-space deuteron wave function with that obtained from the CD-Bonn potential is remarkable, especially in the S-wave.

Finally we obtain the coordinate space wave functions by Fourier transformation

$$\frac{u_L(r)}{r} = \sqrt{\frac{2}{\pi}} \int dp p^2 j_L(pr) \psi_L(p), \quad (4.11)$$

where j_L is the spherical Bessel function, with $L = 0$ for the 3S_1 wave and $L = 2$ for the 3D_1 wave. In bottom part of Fig. 10 the wave functions $u(r) \equiv u_0(r)$ and $w(r) \equiv u_2(r)$ are shown as a function of r . We see that our coordinate-space wave functions have a node near the origin, which is due to the fact that the LO χ PT potential has additional bound states at larger values of B , i.e. the $B = 2.1$ MeV state is not the ground state. The short-distance behavior of the deuteron wave function obtained from the LO χ PT potential has been derived analytically, and discussed in considerable detail, in Ref. [35]. Our results for $u(r)$ and $w(r)$ at the distances where the Fourier transform is numerically stable appear to be in agreement with that work.

In fact, Figs. 8 and 9 show that for this value of the cutoff another eigenvalue crosses 1 at $B = 1.76$ GeV. This is the binding energy of the second-shallowest bound state for $\Lambda = 50000$ MeV; B for this state is slightly smaller at lower cutoffs. The binding momentum of this state is about 1.2 GeV, and so this state is outside the radius of convergence of χ PT: the theory's prediction of its existence is not reliable, and should be disregarded. For completeness, we show the wave function corresponding to this binding energy in Fig. 11. The momentum distribution confirms that the prediction of this state by the low-momentum effective theory is not reliable.

V. SUMMARY AND CONCLUSIONS

We have developed a subtractive renormalization of the S-wave Lippmann-Schwinger equation for the leading-order NN potential of χ PT. Our results are equivalent to earlier work where the contact interaction in NN S-waves was fitted to obtain a particular scattering length. The advantage of our subtraction formulation is that all reference to the unphysical, regularization- and renormalization-dependent contact interaction C disappears from the scattering equation. Instead of searching for the unknown constants C_S and C_T , we directly use the NN scattering lengths a_s and a_t as input and thereby obtain low-energy phase shifts as well as the spectrum and wave functions of all NN bound states which are within the domain of validity of χ PT. Finding C_S and C_T for large cutoffs Λ can be numerically challenging. Subtractive renormalization avoids this problem, and so allows us to compute NN phase shifts from the LO χ PT potential up to $\Lambda = 50$ GeV—a factor of 10 larger than previously employed in momentum-space calculations.

The subtractive technique hence yields phase shifts—and bound-state information—based only on four assumptions:

1. The form of the long-range potential (in this case assumed to be one-pion exchange);
2. The validity of the Lippmann-Schwinger equation;
3. Hermiticity of the underlying NN potential;
4. Energy independence of the short-distance piece of the NN potential—or at least approximate energy dependence over the range of energies considered.

Our results therefore rest on fewer assumptions than were employed to get NN phase shifts in the subtractive approach of Ref. [23]. In particular, we do not assume that the Born approximation is valid for the unregulated NN potential (2.1).

We have chosen to develop a subtraction based on using the NN scattering lengths as input. In principle experimental data at any energy for which the effective theory is valid could be used to determine $T(p_0, p_0; E)$ ($p_0^2 = ME$), however, $E = 0$ seems a natural choice since it introduces the NN low-energy parameters directly into the LS equations for the s-waves. This freedom to choose the subtraction point was exploited to develop Callan-Symanzik-type renormalization-group equations for the NN system in Refs. [23, 24].

For higher partial waves such as the NN P-waves (3P_0 , 3P_1 , 3P_2 - 3F_2), we expect that similar logic will allow us to obtain subtractive equations there too. Furthermore, if we include the two-pion exchange potential [6, 7], which is the dominant correction to one-pion exchange in the χ PT expansion for the NN potential, then we might hope that our results for phase shifts will be valid to higher energies. The subtraction technique will still allow us to renormalize the scattering equation for this long-range potential, as long as the assumption that the constant C is approximately energy independent is still valid over the energy range considered (see also Refs. [29, 36]). The ability of subtractive renormalization to facilitate higher-order calculations in this way has already been demonstrated in the three-body problem in an effective field theory with contact interactions alone [37, 38].

Acknowledgments

This work was funded by the US Department of Energy under grant DE-FG02-93ER40756. C. E. and D. P. thank the Department of Energy's Institute for Nuclear Theory at the University of Washington for its hospitality during the initial stages of the writing of this paper. We also thank Enrique Ruiz Arriola and Manuel Pavon Valderrama for illuminating explanations of their results and for comments on the manuscript. We are also grateful to Lucas Platter for a careful reading of the manuscript.

-
- [1] S. Weinberg, *Physica A* **96**, 327 (1979).
 - [2] J. Gasser and H. Leutwyler, *Nucl. Phys. B* **250**, 465 (1985); *Annals Phys.* **158**, 142 (1984).
 - [3] V. Bernard, N. Kaiser, and U.-G. Meißner, *Int. J. Mod. Phys. E* **4**, 193 (1995).
 - [4] S. Weinberg, *Phys. Lett. B* **251**, 288 (1990).
 - [5] S. Weinberg, *Nucl. Phys. B* **363**, 3 (1991);
 - [6] C. Ordóñez, L. Ray and U. van Kolck, *Phys. Rev. C* **53**, 2086 (1996).
 - [7] N. Kaiser, R. Brockmann and W. Weise, *Nucl. Phys. A* **625**, 758 (1997).
 - [8] E. Epelbaum, W. Glöckle, and U.-G. Meißner, *Nucl. Phys. A* **671**, 295 (2000).
 - [9] D. R. Entem and R. Machleidt, *Phys. Rev. C* **68**, 041001(R) (2003).
 - [10] E. Epelbaum, W. Glöckle and Ulf-G. Meißner, *Nucl. Phys. A* **747**, 362 (2005).
 - [11] G. P. Lepage, arXiv:hep-ph/0506330.
 - [12] G. P. Lepage, arXiv:nucl-th/9706029.
 - [13] S. R. Beane, P. F. Bedaque, M. J. Savage, and U. van Kolck, *Nucl. Phys. A* **700**, 377 (2002).
 - [14] M. P. Valderrama and E. R. Arriola, *Phys. Rev. C* **70**, 044006 (2004).
 - [15] A. Nogga, R.G.E. Timmermans and U. van Kolck, *Phys. Rev. C* **72**, 054006 (2005).
 - [16] M. Pavon Valderrama and E. Ruiz Arriola, *Phys. Rev. C* **74**, 064004 (2006).
 - [17] M. C. Birse, *Phys. Rev. C* **74**, 014003 (2006).
 - [18] E. Epelbaum and Ulf-G. Meißner, arXiv:nucl-th/0609037.
 - [19] H.-W. Hammer, N. Kalantar-Nayestanaki and D. R. Phillips, arXiv:nucl-th/0611084.
 - [20] See, for example, C. Itzykson and J.-B. Zuber, *Quantum Field Theory* (McGraw-Hill, Singapore, 1985), pp. 389–394, and references therein.
 - [21] H.-W. Hammer and T. Mehen, *Nucl. Phys. A* **690**, 535 (2001).
 - [22] I. R. Afnan and D. R. Phillips, *Phys. Rev. C* **69**, 034010 (2004).
 - [23] T. Frederico, V. S. Timoteo and L. Tomio, *Nucl. Phys. A* **653**, 209 (1999).
 - [24] V. S. Timoteo, T. Frederico, A. Delfino and L. Tomio, *Phys. Lett. B* **621**, 109 (2005).
 - [25] S. R. Beane, P. F. Bedaque, K. Orginos and M. J. Savage, *Phys. Rev. Lett.* **97**, 012001 (2006).
 - [26] M.I. Haftel and F. Tabakin, *Nucl. Phys. A* **158**, 1 (1970).
 - [27] V. G. J. Stoks, R. A. M. Klomp, C. P. F. Terheggen and J. J. de Swart, *Phys. Rev. C* **49**, 2950 (1994).
 - [28] R. Machleidt, *Phys. Rev. C* **63**, 024001 (2001).
 - [29] M. Pavon Valderrama, and E. Ruiz Arriola, *Phys. Rev. C* **74**, 054001 (2006).
 - [30] H. P. Stapp, T. J. Ypsilantis and N. Metropolis, *Phys. Rev.* **105**, 302 (1957).
 - [31] B. D. Keister and W. N. Polyzou, *Phys. Rev. C* **73**, 014005 (2006).
 - [32] T. Lin, C. Elster, W. N. Polyzou and W. Glöckle, *Phys. Rev. C* **76**, 014010 (2007).
 - [33] M. L. Goldberger and K. M. Watson, *Collision Theory* (Wiley, New York, 1964), pp. 306–309.
 - [34] Ch. Zemach, A. Klein, *Nuov. Cim.* **10**, 1078 (1958).
 - [35] M. P. Valderrama and E. R. Arriola, *Phys. Rev. C* **72**, 054002 (2005).
 - [36] M. C. Birse, arXiv:0706.984 [nucl-th].
 - [37] L. Platter and D. R. Phillips, *Few Body Syst.* **40**, 35 (2006).
 - [38] L. Platter, *Phys. Rev. C* **74**, 037001 (2006).

Λ [MeV]	r_s [fm]	r_t [fm]
500	1.556	1.582
1000	1.441	1.614
5000	1.365	1.596
10000	1.356	1.595
50000	1.349	1.594

TABLE I: Effective range r_s (singlet) and r_t (triplet) obtained using the method of Section 2 for various cutoffs Λ .

Λ [MeV]	C_S [MeV $^{-2}$]	C_T [MeV $^{-2}$]
500	-6.069×10^{-6}	-2.307×10^{-6}
1000	-4.926×10^{-6}	-1.838×10^{-5}
5000	-3.902×10^{-6}	1.310×10^{-6}
10000	-3.753×10^{-6}	2.040×10^{-5}
50000	-3.627×10^{-6}	-4.201×10^{-8}

TABLE II: The constants C_S and C_T as determined by fitting the scattering lengths a_s and a_t for different cutoff parameters Λ .

Mesh points	$\delta(^3S_1)$ Fitting	$\delta(^3S_1)$ Subtraction
20	139.2453	104.6811
30	113.8653	104.6649
40	107.9943	104.6622
50	105.9794	104.6618
100	104.2317	104.6616
150	104.0749	104.6616

TABLE III: The convergence of the phase shift $\delta(^3S_1)$ at laboratory kinetic energy $T_{lab}=10$ MeV as a function of the number of Gauss-Legendre quadratures for the fitting and subtraction methods. Note that the fitting method converges to 104.1 at about 200 mesh points, so the final results of these two methods differ by $\approx 0.5\%$ as per Fig. 5.

Λ [MeV]	B_{fit} [MeV]	B_{sub} [MeV]
500	2.10	2.11
1000	2.12	2.11
5000	2.11	2.11
10000	2.11	2.11
50000	2.13	2.11

TABLE IV: The binding energy B for different cutoff parameters Λ . The binding energy B_{fit} is obtained from the fitting method described in Section 2, and the binding energy B_{sub} is obtained from the subtractive method given in Section 3.

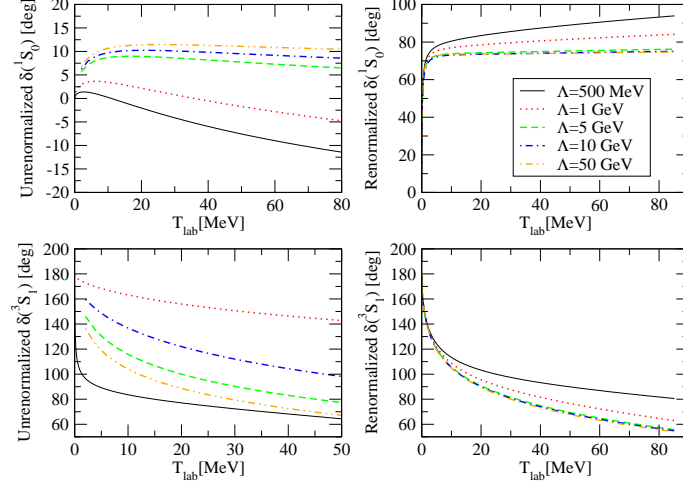


FIG. 1: (Color online) The NN phase shift $\delta(^1S_0)$ and $\delta(^3S_1)$ as function of the laboratory kinetic energy $T_{\text{lab}} \leq 80$ MeV for cutoff parameters Λ ranging from 0.5–50 GeV. The upper left panel shows the phase shift with $C_S = 0$, while the upper right panel shows the value with C_S adjusted at each value of Λ to reproduce the experimental value of a_s . The bottom left panel shows the phase shift with $C_T = 0$, while the bottom right panel shows the value with C_T adjusted at each value of Λ to reproduce the experimental value of a_t . Note that the phase shift in both lower panels is given modulo π only, since multiple deeply bound states are present.

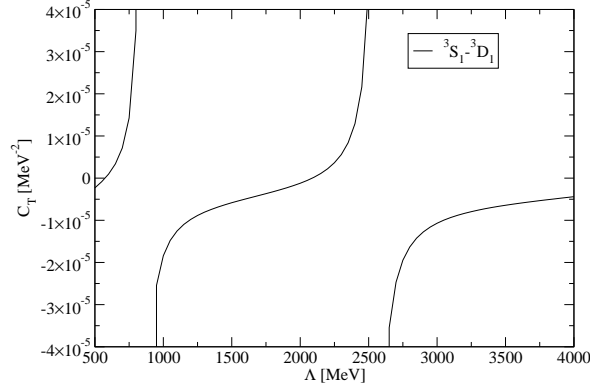


FIG. 2: The renormalization constant C_T for the triplet channel as a function of the cutoff Λ , where Λ ranges from 0.5–4 GeV.

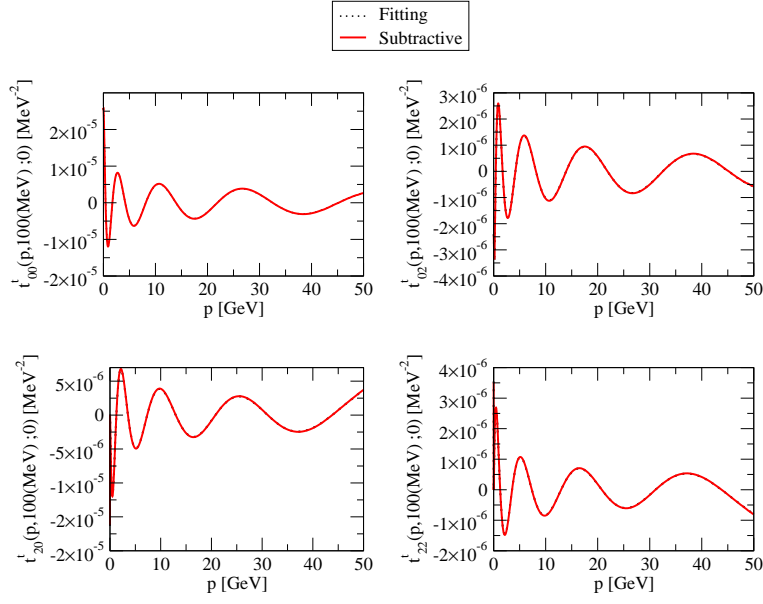


FIG. 3: (Color online) The comparison of the two renormalization methods for zero energy off-shell matrix element $t_W(p, p'; 0)$ in the triplet channel as a function of the momentum p for fixed $p' = 100$ MeV.

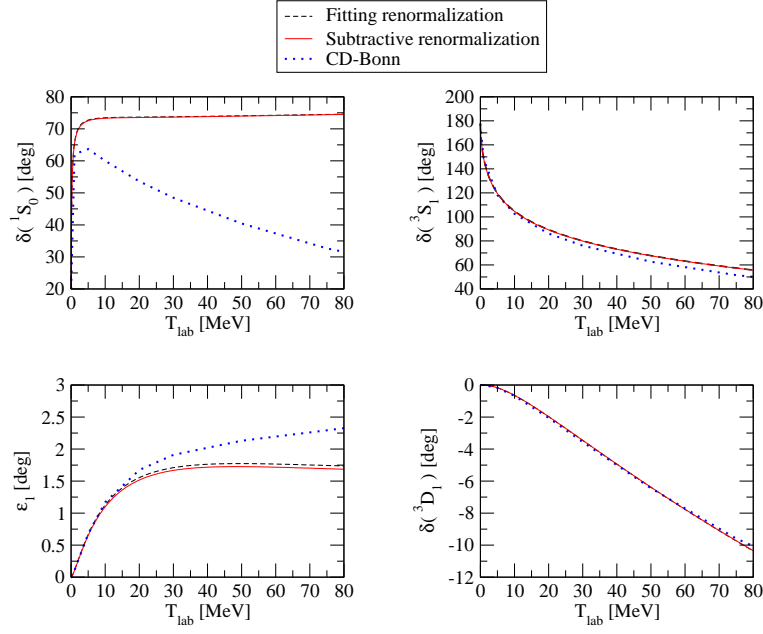


FIG. 4: (Color online) The comparison of two renormalization methods for the lowest NN singlet and triplet phase shifts and mixing parameter as a function of the laboratory kinetic energy $T_{\text{lab}} \leq 80$ MeV. Here $\Lambda = 50$ GeV is used. The phase shifts obtained from the CD-Bonn potential are also shown (dashed lines).

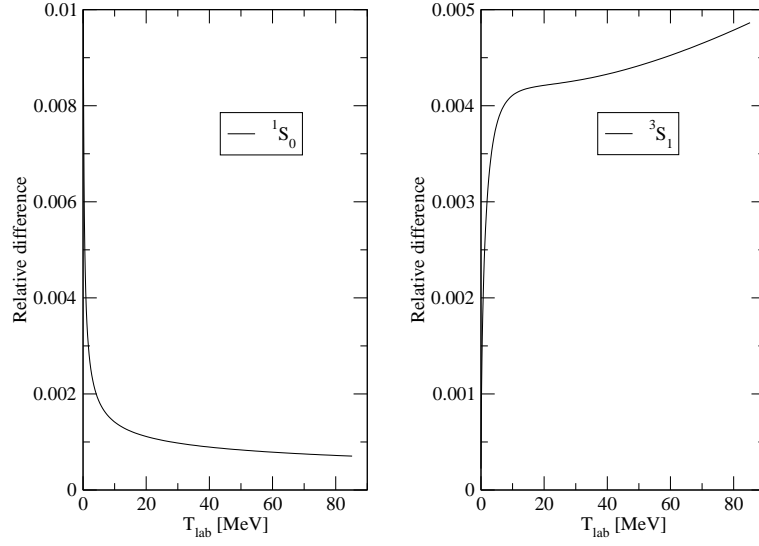


FIG. 5: The relative difference of NN $\delta(^1S_0)$ and $\delta(^3S_1)$ phase shift between two renormalization methods as a function of the laboratory kinetic energy $T_{\text{lab}} \leq 80$ MeV. Here $\Lambda = 50$ GeV is used, and 100 Gauss-Legendre quadrature points are chosen for the solution of the LS equation.

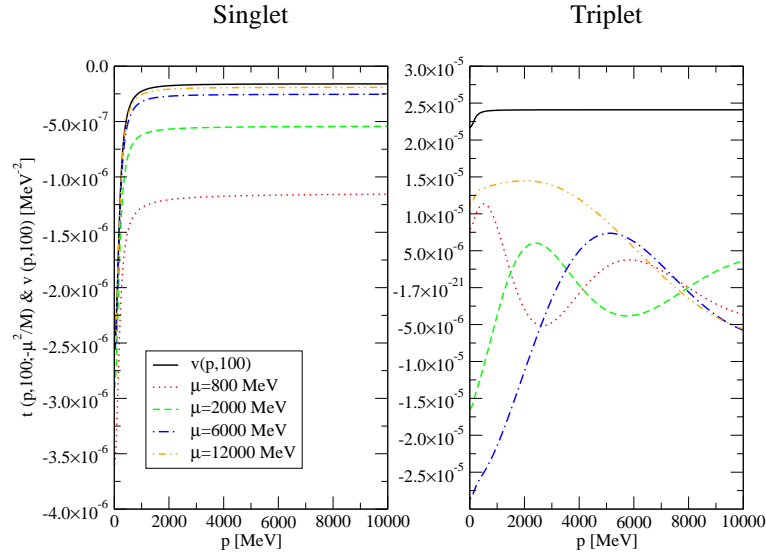


FIG. 6: The t-matrix elements $t^s(p, 100; -\frac{\mu^2}{M})$ (left) and $t_{00}^t(p, 100; -\frac{\mu^2}{M})$ (right) as functions of the half-shell momentum p compared to $v^s(p, 100)$ and $v_{00}^t(p, 100)$. The parameter μ ranges from 0.8–12 GeV.

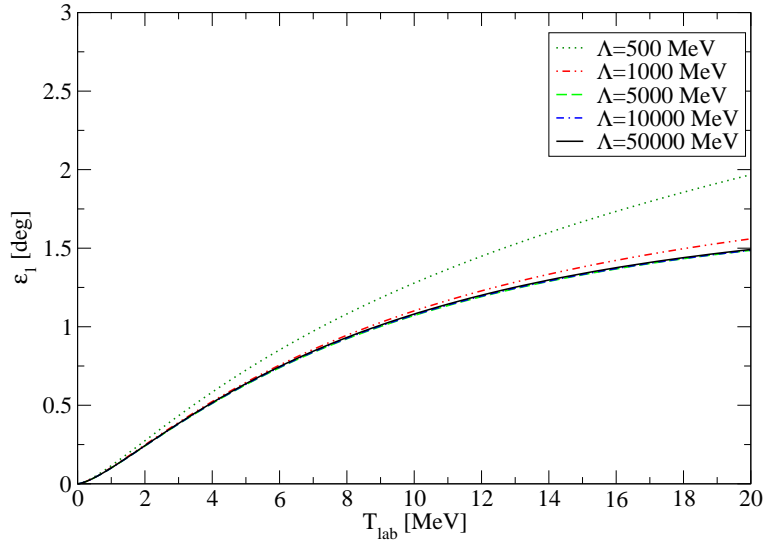


FIG. 7: The mixing parameter ϵ_1 obtained with the subtraction method as a function of the laboratory kinetic energy $T_{\text{lab}} \leq 20$ MeV and for cutoff parameters Λ ranging from 0.5–50 GeV.

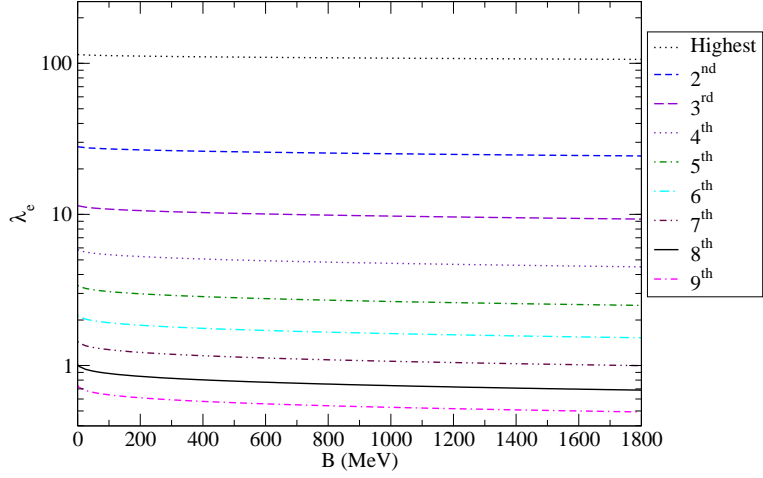


FIG. 8: (Color online) The eigenvalues λ_e obtained from Eq. (4.3) as a function of the binding energy B . Note that the vertical axis is on a log scale.

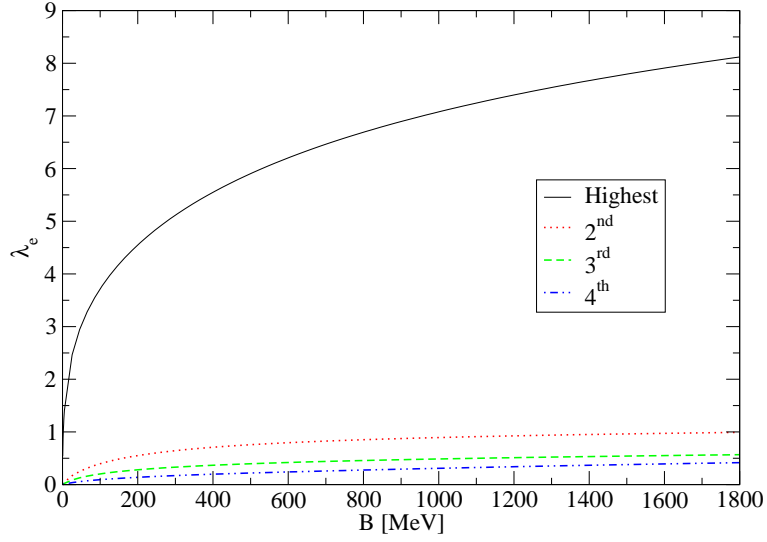


FIG. 9: (Color online) The eigenvalues λ_e obtained from Eq. (4.5) as a function of the binding energy B .

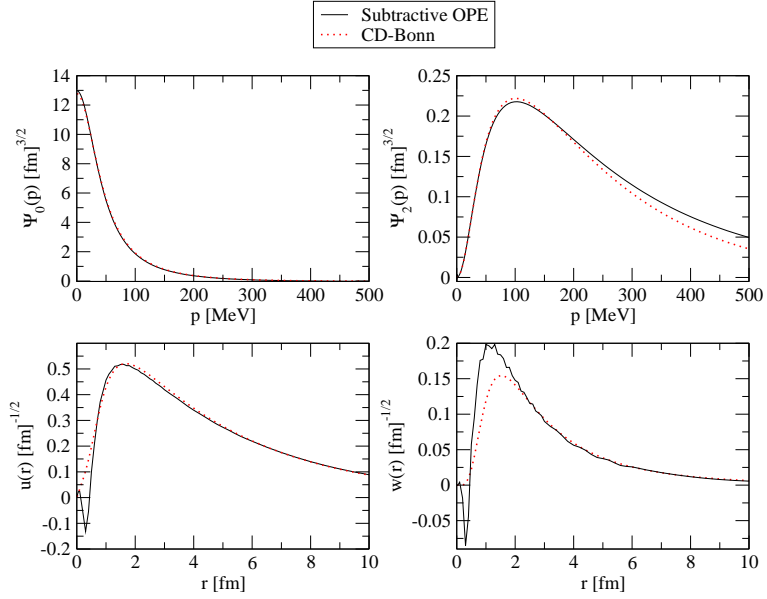


FIG. 10: (Color online) Upper panel shows the momentum-space wave functions of the shallowest NN bound state in the triplet channel as a function of p , where $\psi_0(p)$ is the 3S_1 wave function and $\psi_2(p)$ denotes the 3D_1 wave (solid lines). These wave functions are obtained from the subtracted integral equation with $\Lambda = 50$ GeV. Bottom panel shows the coordinate-space wave functions as functions of r , where $u(r)$ denotes the 3S_1 wave and $w(r)$ denotes the 3D_1 wave (solid lines). The dotted lines indicate the corresponding wave functions obtained from the CD-Bonn potential.

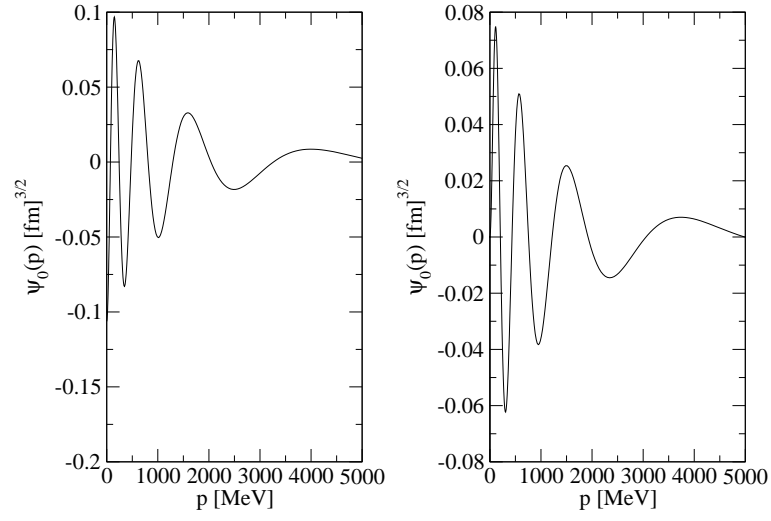


FIG. 11: Wave functions of the second-shallowest NN bound state in the triplet channel as functions of p , where $\psi_0(p)$ denotes the 3S_1 wave and $\psi_2(p)$ denotes the 3D_1 wave. These wave functions are obtained from the subtracted integral equation with $\Lambda = 50$ GeV.